

# Comparison of lithium nickel cobalt oxides synthesized from NiO, Co<sub>3</sub>O<sub>4</sub>, and LiOH·H<sub>2</sub>O or Li<sub>2</sub>CO<sub>3</sub> by solid-state reaction method

Eui Yong Bang<sup>a</sup>, Daniel R. Mumm<sup>b</sup>, Hye Ryoung Park<sup>c</sup>, Myoung Youp Song<sup>d,\*</sup>

<sup>a</sup> Hanwha Chemical Research & Development Center, 6 Shinseong-Dong Yuseong-Gu Daejeon, 305-804, Republic of Korea

<sup>b</sup> Department of Chemical Engineering and Materials Science, University of California Irvine, Irvine, CA 92697-2575, USA

<sup>c</sup> School of Applied Chemical Engineering, Chonnam National University, 300 Yongbong-Dong Buk-Gu Gwangju, 500-757, Republic of Korea

<sup>d</sup> Division of Advanced Materials Engineering, Hydrogen & Fuel Cell Research Center, Engineering Research Institute, Chonbuk National University, 567 Baekje-Daero Deokjin-Gu Jeonju, 561-756, Republic of Korea

Received 6 March 2012; accepted 3 April 2012

Available online 12 April 2012

## Abstract

LiNi<sub>1-y</sub>Co<sub>y</sub>O<sub>2</sub> ( $y = 0.1, 0.3$  and  $0.5$ ) cathode materials were synthesized by the solid-state reaction method at different temperatures from LiOH·H<sub>2</sub>O, NiO and Co<sub>3</sub>O<sub>4</sub> and from Li<sub>2</sub>CO<sub>3</sub>, NiO and Co<sub>3</sub>O<sub>4</sub> as the starting materials. The physical and electrochemical properties of the synthesized samples were then compared. Among LiNi<sub>1-y</sub>Co<sub>y</sub>O<sub>2</sub> ( $y = 0.1, 0.3$  and  $0.5$ ) synthesized for 40 h from LiOH·H<sub>2</sub>O, NiO and Co<sub>3</sub>O<sub>4</sub>, and from Li<sub>2</sub>CO<sub>3</sub>, NiO and Co<sub>3</sub>O<sub>4</sub>, LiNi<sub>0.5</sub>Co<sub>0.5</sub>O<sub>2</sub> synthesized from Li<sub>2</sub>CO<sub>3</sub>, NiO and Co<sub>3</sub>O<sub>4</sub> at 800 °C has relatively large first discharge capacity and relatively good cycling performance. This sample is considered the best one with relatively good electrochemical properties.

© 2012 Elsevier Ltd and Techna Group S.r.l. All rights reserved.

**Keywords:** LiNi<sub>1-y</sub>Co<sub>y</sub>O<sub>2</sub>; Solid-state reaction method; LiOH·H<sub>2</sub>O or Li<sub>2</sub>CO<sub>3</sub>; Degree of displacement of the nickel and lithium ions; Discharge capacity; Capacity fading rate

## 1. Introduction

LiCoO<sub>2</sub> [1–3], LiNiO<sub>2</sub> [4–8], and LiMn<sub>2</sub>O<sub>4</sub> [9–14] have been investigated as cathode materials for lithium secondary batteries [15]. LiMn<sub>2</sub>O<sub>4</sub> is relatively cheap and environment-friendly, but its cycling performance is poor. LiCoO<sub>2</sub> has a large diffusivity and a high operating voltage, and its preparation is easy. However, it has a disadvantage that it contains an expensive element, Co.

LiNiO<sub>2</sub> has a large discharge capacity [16] and is relatively excellent from the viewpoints of economics and environment. It is thus considered a very promising cathode material. However, since the sizes of Li and Ni ions ( $\text{Li}^+ = 0.72 \text{ \AA}$  and  $\text{Ni}^{2+} = 0.69 \text{ \AA}$ ) are similar, the LiNiO<sub>2</sub> is practically obtained in the non-stoichiometric composition, Li<sub>1-y</sub>Ni<sub>1+y</sub>O<sub>2</sub> [17,18]. The Ni<sup>2+</sup> ions in the lithium planes obstruct the movement of the Li<sup>+</sup> ions during charge and discharge [19,20].

Since the presence of cobalt stabilizes the structure in a strictly two-dimensional fashion, incorporation of LiCoO<sub>2</sub> and LiNiO<sub>2</sub> phases into LiNi<sub>1-y</sub>Co<sub>y</sub>O<sub>2</sub> favors good reversibility of the intercalation and deintercalation reactions [19,21–28]. Rougier et al. [19] reported that the stabilization of the two-dimensional character of the structure by cobalt substitution in LiNiO<sub>2</sub> is correlated with an increase in the cell performance, due to the decrease in the amount of extra-nickel ions in the inter-slab space which impede the lithium diffusion.

In our previous work [29], we studied the electrochemical properties of the cathode materials, LiNi<sub>1-y</sub>Co<sub>y</sub>O<sub>2</sub>, synthesized from LiOH·H<sub>2</sub>O or Li<sub>2</sub>CO<sub>3</sub>, NiO or NiCO<sub>3</sub>, and Co<sub>3</sub>O<sub>4</sub> or CoCO<sub>3</sub> by the solid-state reaction method. The cathode materials, LiNi<sub>1-y</sub>Co<sub>y</sub>O<sub>2</sub>, synthesized from LiOH·H<sub>2</sub>O, NiO and Co<sub>3</sub>O<sub>4</sub>, and from Li<sub>2</sub>CO<sub>3</sub>, NiO and Co<sub>3</sub>O<sub>4</sub> showed relatively good electrochemical properties.

In this work, LiNi<sub>1-y</sub>Co<sub>y</sub>O<sub>2</sub> ( $y = 0.1, 0.3$  and  $0.5$ ) cathode materials were synthesized by the solid-state reaction method at different temperatures from LiOH·H<sub>2</sub>O, NiO and Co<sub>3</sub>O<sub>4</sub>, and from Li<sub>2</sub>CO<sub>3</sub>, NiO and Co<sub>3</sub>O<sub>4</sub> as the starting materials. The physical and electrochemical properties of the synthesized samples were then compared.

\* Corresponding author. Tel.: +82 63 270 2379; fax: +82 63 270 2386.

E-mail address: [songmy@jbnu.ac.kr](mailto:songmy@jbnu.ac.kr) (M.Y. Song).

## 2. Experimental

LiOH·H<sub>2</sub>O (High Purity Chemical Laboratory Co., purity 99%), Li<sub>2</sub>CO<sub>3</sub> (High Purity Chemical Laboratory Co., purity 99%), NiO (High Purity Chemical Laboratory Co., purity 99.9%) and Co<sub>3</sub>O<sub>4</sub> (High Purity Chemical Laboratory Co., purity 99.9%) were used as the starting materials in order to synthesize LiNi<sub>1-y</sub>Co<sub>y</sub>O<sub>2</sub> by the solid-state reaction method.

The mixture of starting materials in the compositions LiNi<sub>1-y</sub>Co<sub>y</sub>O<sub>2</sub> ( $y = 0.1, 0.3$  and  $0.5$ ) was mixed and pelletized. This pellet was heat-treated in air at 650 °C for 20 h, and was then ground, mixed, pelletized again and calcined at 750 °C, 800 °C or 850 °C for 20 h. This pellet was cooled at a cooling rate of 50 °C/min, ground, mixed and pelletized again. It was then calcined again at 750 °C, 800 °C or 850 °C for 20 h.

The phase identification of the synthesized samples was carried out by X-ray diffraction (XRD) analysis with Cu K $\alpha$  radiation using a Rigaku type III/A X-ray diffractometer. The scanning rate was 4°/min and the scanning range of the diffraction angle ( $2\theta$ ) was  $10^\circ \leq 2\theta \leq 70^\circ$ . The morphologies of the samples were observed using a scanning electron microscope (SEM) or a field emission scanning electron microscope (FE-SEM).

The electrochemical cells consisted of LiNi<sub>1-y</sub>Co<sub>y</sub>O<sub>2</sub> as a positive electrode, Li foil as a negative electrode, and an electrolyte [Purelyte (Samsung Chemicals Ltd.)] prepared by dissolving 1 M LiPF<sub>6</sub> in a 1:1(volume ratio) mixture of ethylene carbonate (EC) and dimethyl carbonate (DMC). A Whatman glass-fiber was used as the separator. To fabricate the positive electrode, 89 wt% synthesized oxide, 10 wt% acetylene black and 1 wt% polytetrafluoroethylene (PTFE) binder were mixed in an agate mortar. The cell was assembled in a glove box filled with argon. All of the electrochemical tests were performed at room temperature with a potentiostatic/galvanostatic system. The cells were cycled at a current density of 200  $\mu\text{A}/\text{cm}^2$  between 3.2 and 4.3 V.

## 3. Results and discussion

Fig. 1 shows the X-ray diffraction (XRD) patterns of LiNi<sub>1-y</sub>Co<sub>y</sub>O<sub>2</sub> ( $y = 0.1, 0.3$  and  $0.5$ ) powders synthesized at 800 °C for 20 h from LiOH·H<sub>2</sub>O, NiO and Co<sub>3</sub>O<sub>4</sub>. They are identified as corresponding to the  $\alpha$ -NaFeO<sub>2</sub> structure of the rhombohedral system (space group;  $R\bar{3}m$ ). The diffraction angles of the peaks corresponding to this structure increase as the content of Co increases. Impurity peaks appear at the diffraction angles  $2\theta = 21^\circ$  and  $32^\circ$ . These peaks were identified as those of the Li<sub>2</sub>CO<sub>3</sub> phase. As the Co content increases, the intensities of these peaks decrease.

The SEM micrographs of LiNi<sub>1-y</sub>Co<sub>y</sub>O<sub>2</sub> ( $y = 0.1, 0.3$  and  $0.5$ ) synthesized at 800 °C for 20 h from LiOH·H<sub>2</sub>O, NiO and Co<sub>3</sub>O<sub>4</sub> are shown in Fig. 2. The samples consist of large and small particles. Some large particles are agglomerated. As Co content increases, particles get larger.

Fig. 3 presents the SEM micrographs of LiNi<sub>1-y</sub>Co<sub>y</sub>O<sub>2</sub> ( $y = 0.1, 0.3$  and  $0.5$ ) synthesized at 800 °C for 20 h from

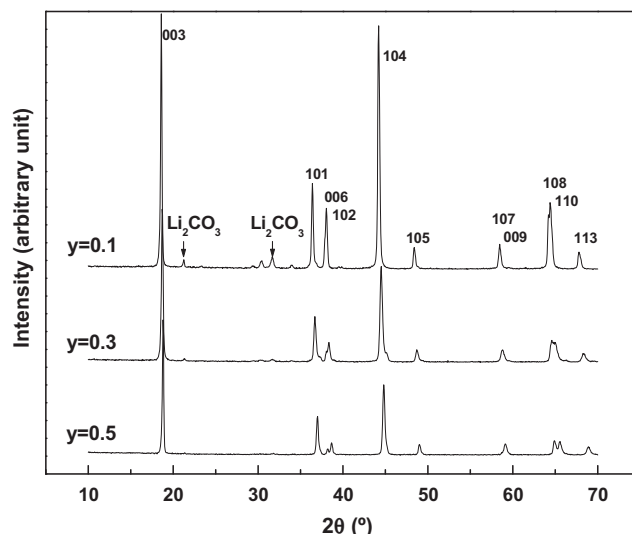


Fig. 1. XRD patterns of LiNi<sub>1-y</sub>Co<sub>y</sub>O<sub>2</sub> ( $y = 0.1, 0.3$  and  $0.5$ ) powders synthesized at 800 °C for 20 h from LiOH·H<sub>2</sub>O, NiO and Co<sub>3</sub>O<sub>4</sub>.

Li<sub>2</sub>CO<sub>3</sub>, NiO and Co<sub>3</sub>O<sub>4</sub>. The forms of particles are irregular and the particle sizes are not homogeneous. Some particles are agglomerated. These particles are a little larger than those synthesized from LiOH·H<sub>2</sub>O, NiO and Co<sub>3</sub>O<sub>4</sub> in Fig. 2.

The XRD patterns of LiNi<sub>1-y</sub>Co<sub>y</sub>O<sub>2</sub> ( $y = 0.1, 0.3$  and  $0.5$ ) powders synthesized at 750 °C for 40 h from Li<sub>2</sub>CO<sub>3</sub>, NiO and Co<sub>3</sub>O<sub>4</sub> are exhibited in Fig. 4. They are identified as corresponding to the  $\alpha$ -NaFeO<sub>2</sub> structure of the rhombohedral system (space group;  $R\bar{3}m$ ). The diffraction angles of the peaks corresponding to this structure increase as the content of Co increases. Li<sub>2</sub>CO<sub>3</sub> peaks appear at the diffraction angles  $2\theta = 21^\circ$  and  $32^\circ$ . As the Co content increases, the intensities of these peaks decrease.

Fig. 5 presents the variations of intensity ratio of 0 0 3 and 1 0 4 peaks,  $I_{003}/I_{104}$ , with  $y$  in LiNi<sub>1-y</sub>Co<sub>y</sub>O<sub>2</sub> synthesized at 800 °C for 20 h or 40 h using NiO, Co<sub>3</sub>O<sub>4</sub>, and LiOH·H<sub>2</sub>O or Li<sub>2</sub>CO<sub>3</sub> as starting materials. The intensity ratio,  $I_{003}/I_{104}$ , increases as the Co content increases. The 0 0 3 peak originates from the diffraction of only the  $R\bar{3}m$   $\alpha$ -NaFeO<sub>2</sub> structure, while the 1 0 4 peak originates from the diffractions of both the  $R\bar{3}m$   $\alpha$ -NaFeO<sub>2</sub> and  $Fm\bar{3}m$  NaCl structures. Therefore, it is possible to calculate the fraction of each phase from the intensity ratio of the 0 0 3 and 1 0 4 peaks. Morales et al. [18] reported that the intensity ratio,  $I_{003}/I_{104}$ , of the completely stoichiometric composition LiNiO<sub>2</sub> is about 1.3. The LiNi<sub>0.7</sub>Co<sub>0.3</sub>O<sub>2</sub> specimen synthesized for 40 h from LiOH·H<sub>2</sub>O, NiO and Co<sub>3</sub>O<sub>4</sub>, and the LiNi<sub>0.5</sub>Co<sub>0.5</sub>O<sub>2</sub> synthesized for 20 h and LiNi<sub>0.7</sub>Co<sub>0.3</sub>O<sub>2</sub> synthesized for 40 h from Li<sub>2</sub>CO<sub>3</sub>, NiO and Co<sub>3</sub>O<sub>4</sub> have  $I_{003}/I_{104}$  values which are nearly 1.3. Ohzuku et al. [30] investigated the factors affecting the electrochemical reactivity of LiNiO<sub>2</sub>. They reported that as the intensity ratio of the 0 0 3 and 1 0 4 peaks increases, the degree of displacement of the nickel and lithium ions decreases. The disordered region prevents the extension and reduction of the interlayer distance between the NiO<sub>2</sub> sheets, making sliding between the basal planes impossible. Consequently, the nickel ions in the lithium

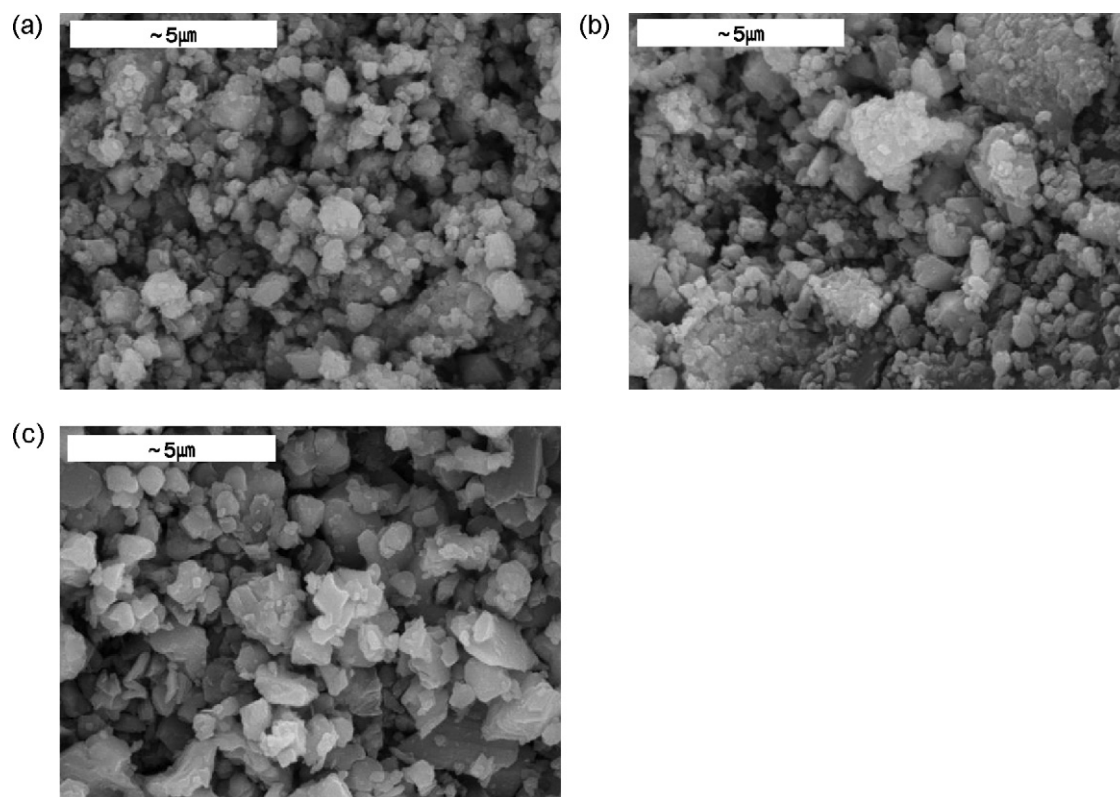


Fig. 2. SEM micrographs of  $\text{LiNi}_{1-y}\text{Co}_y\text{O}_2$  synthesized at 800 °C for 20 h from  $\text{LiOH}\cdot\text{H}_2\text{O}$ ,  $\text{NiO}$  and  $\text{Co}_3\text{O}_4$ : (a)  $y = 0.1$ , (b)  $y = 0.3$  and (c)  $y = 0.5$ .

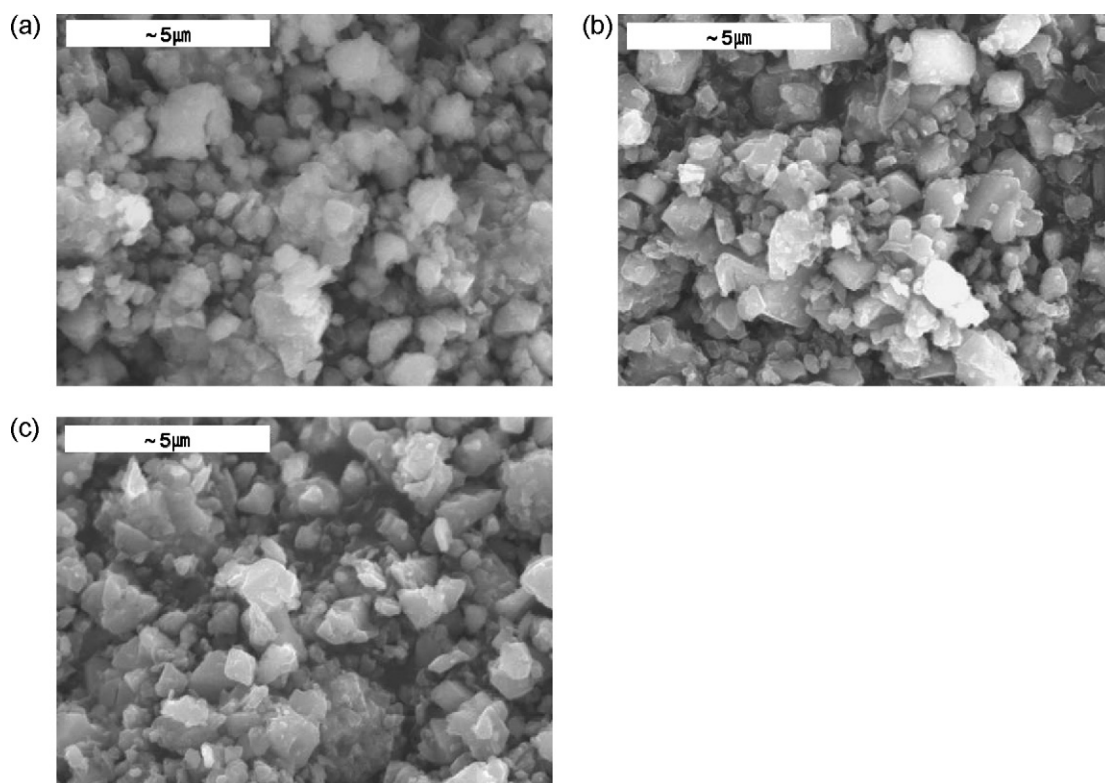


Fig. 3. SEM micrographs of  $\text{LiNi}_{1-y}\text{Co}_y\text{O}_2$  synthesized at 800 °C for 20 h from  $\text{Li}_2\text{CO}_3$ ,  $\text{NiO}$  and  $\text{Co}_3\text{O}_4$ : (a)  $y = 0.1$ , (b)  $y = 0.3$  and (c)  $y = 0.5$ .

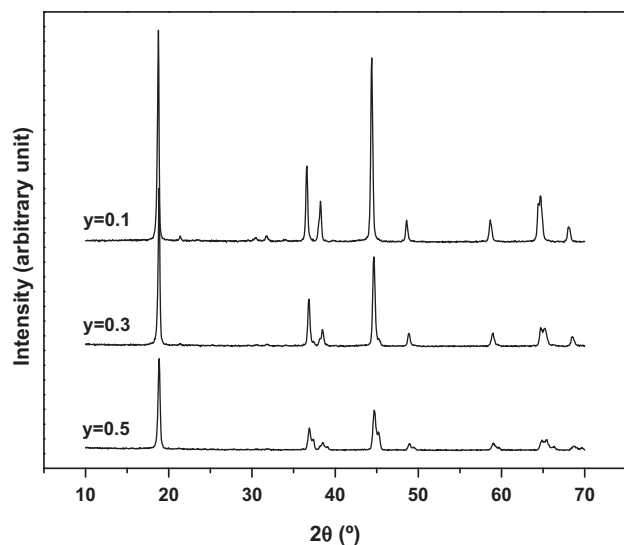


Fig. 4. XRD patterns of  $\text{LiNi}_{1-y}\text{Co}_y\text{O}_2$  ( $y = 0.1, 0.3$  and  $0.5$ ) powders synthesized at  $750^\circ\text{C}$  for 40 h from  $\text{Li}_2\text{CO}_3$ ,  $\text{NiO}$  and  $\text{Co}_3\text{O}_4$ .

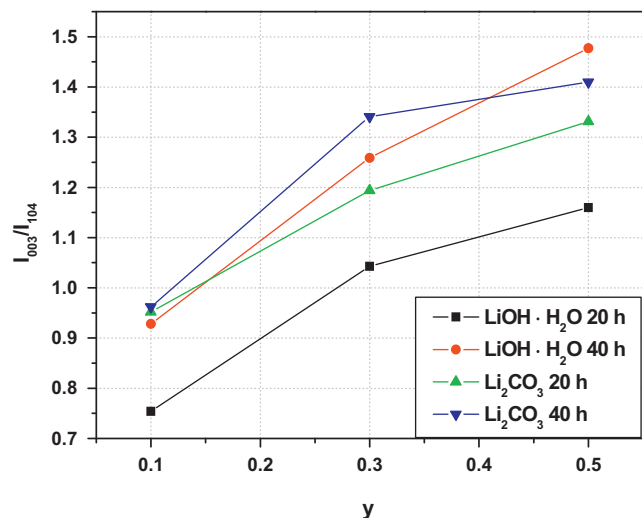


Fig. 5. Variations of intensity ratio of 003 and 104 peaks,  $I_{003}/I_{104}$ , with  $y$  in  $\text{LiNi}_{1-y}\text{Co}_y\text{O}_2$  synthesized at  $800^\circ\text{C}$  for 20 h or 40 h from  $\text{NiO}$ ,  $\text{Co}_3\text{O}_4$ , and  $\text{LiOH}\cdot\text{H}_2\text{O}$  or  $\text{Li}_2\text{CO}_3$ .

sheet including the near neighbors are inactive for the electrochemical reaction. Fig. 5 shows that the intensity ratio,  $I_{003}/I_{104}$ , increases as the Co content increases. This shows that the degree of displacement of the nickel and lithium ions decreases as the Co content increases.

Ohzuku et al. [30] also reported that electroactive  $\text{LiNiO}_2$  showed a clear split of the (108) and (110) lines, which appear in their XRD patterns at the diffraction angle near  $2\theta = 65^\circ$  around. Fig. 1 shows that the splitting of the (108) and (110) lines becomes clearer as the Co content increases.

Dahn et al. [5] defined the intensity ratio,  $R$ , as the relative intensity of the (102, 006) peak near  $2\theta = 38^\circ$  as compared with that of the (101) peak near  $2\theta = 36.5^\circ$ . Their results showed that the intensity ratio,  $R$ , increases as the unit cell volume increases. They also showed that the intensity ratio,  $R$ ,

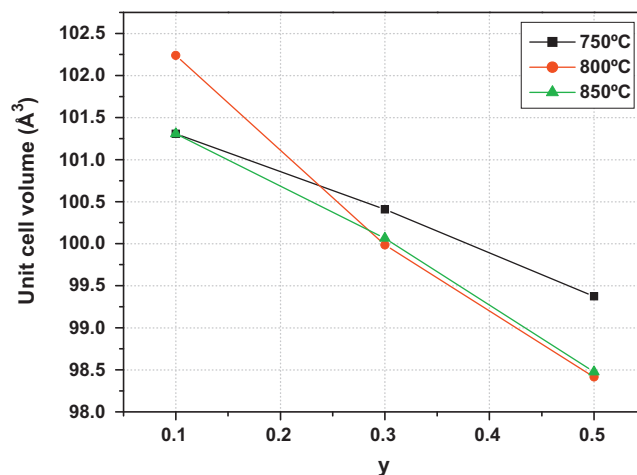


Fig. 6. Variations of unit cell volume with  $y$  in  $\text{LiNi}_{1-y}\text{Co}_y\text{O}_2$  synthesized at  $750, 800$  and  $850^\circ\text{C}$  for 40 h from  $\text{LiOH}\cdot\text{H}_2\text{O}$ ,  $\text{NiO}$  and  $\text{Co}_3\text{O}_4$ .

increases rapidly as  $x$  decreases in  $\text{Li}_x\text{Ni}_{2-x}\text{O}_2$ . This suggests that, as the unit cell volume increases,  $x$  decreases in  $\text{Li}_x\text{Ni}_{2-x}\text{O}_2$ .  $\text{Li}_x\text{Ni}_{2-x}\text{O}_2$  can be expressed as  $(\text{Li}_x\text{Ni}_{1-x})\text{NiO}_2$ . A decrease in  $x$  in  $\text{Li}_x\text{Ni}_{2-x}\text{O}_2$  corresponds to an increase in the degree of displacement of the nickel and lithium ions.

The variations of unit cell volume with  $y$  in  $\text{LiNi}_{1-y}\text{Co}_y\text{O}_2$  (from starting materials  $\text{LiOH}\cdot\text{H}_2\text{O}$ ,  $\text{NiO}$  and  $\text{Co}_3\text{O}_4$ ) synthesized at  $750, 800$  and  $850^\circ\text{C}$  for 40 h are shown in Fig. 6. The variations of unit cell volume with  $y$  in  $\text{LiNi}_{1-y}\text{Co}_y\text{O}_2$  (from starting materials  $\text{Li}_2\text{CO}_3$ ,  $\text{NiO}$  and  $\text{Co}_3\text{O}_4$ ) synthesized at  $750, 800$  and  $850^\circ\text{C}$  for 40 h are presented in Fig. 7. As the value of  $y$  increases, the unit cell volume decreases. This shows that as the Co content increases, the degree of displacement of the nickel and lithium ions decreases.

Fig. 8 presents the FE-SEM micrographs of  $\text{LiNi}_{1-y}\text{Co}_y\text{O}_2$  ( $y = 0.3$  and  $y = 0.5$ ) synthesized at  $800^\circ\text{C}$  for 40 h using  $\text{LiOH}\cdot\text{H}_2\text{O}$ ,  $\text{NiO}$  and  $\text{Co}_3\text{O}_4$  as starting materials. The samples in the shape of polyhedrons consist of small and large particles.  $\text{LiNi}_{0.5}\text{Co}_{0.5}\text{O}_2$  has larger particles than  $\text{LiNi}_{0.7}\text{Co}_{0.3}\text{O}_2$ .

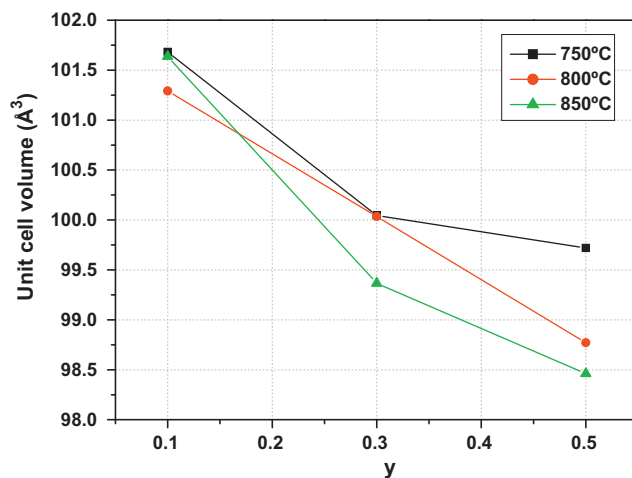


Fig. 7. Variations of unit cell volume with  $y$  in  $\text{LiNi}_{1-y}\text{Co}_y\text{O}_2$  synthesized at  $750, 800$  and  $850^\circ\text{C}$  for 40 h from  $\text{Li}_2\text{CO}_3$ ,  $\text{NiO}$  and  $\text{Co}_3\text{O}_4$ .



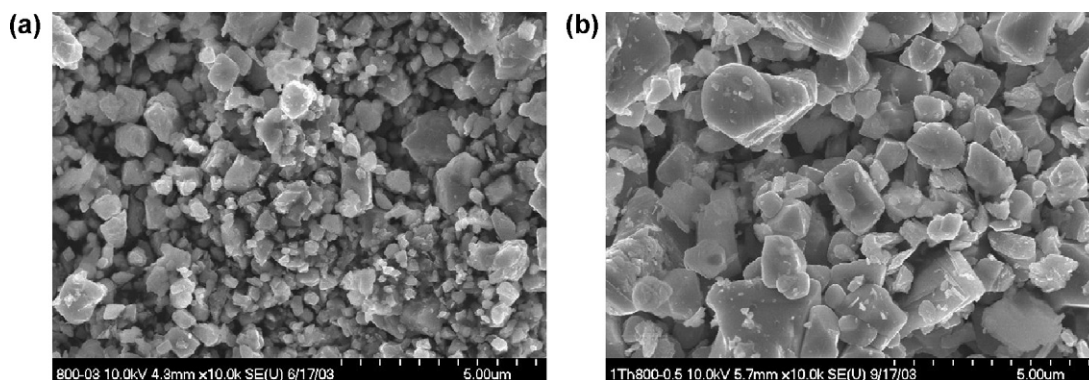


Fig. 8. FE-SEM micrographs of  $\text{LiNi}_{1-y}\text{Co}_y\text{O}_2$  synthesized at 800 °C for 40 h from  $\text{LiOH}\cdot\text{H}_2\text{O}$ , NiO and  $\text{Co}_3\text{O}_4$ : (a)  $y = 0.3$  and (b)  $y = 0.5$ .

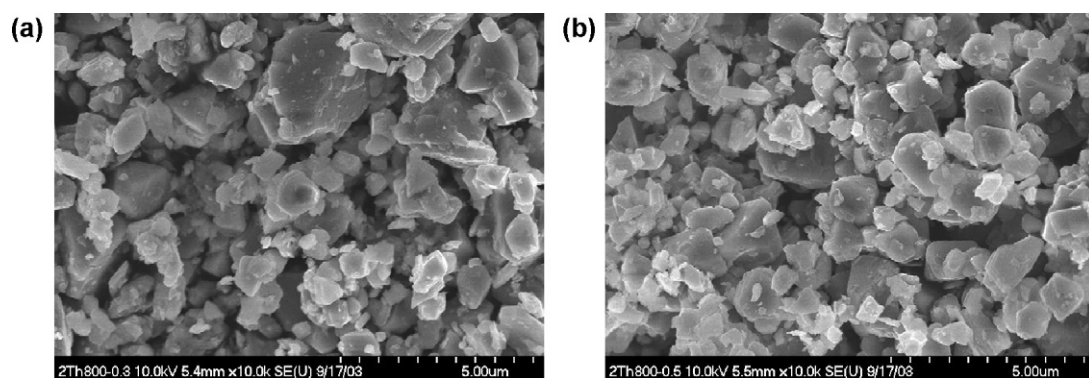


Fig. 9. FE-SEM micrographs of  $\text{LiNi}_{1-y}\text{Co}_y\text{O}_2$  synthesized at 800 °C for 40 h from  $\text{Li}_2\text{CO}_3$ , NiO and  $\text{Co}_3\text{O}_4$ : (a)  $y = 0.3$  and (b)  $y = 0.5$ .

The FE-SEM micrographs of  $\text{LiNi}_{1-y}\text{Co}_y\text{O}_2$  ( $y = 0.3$  and  $y = 0.5$ ) synthesized at 800 °C for 40 h using  $\text{Li}_2\text{CO}_3$ , NiO and  $\text{Co}_3\text{O}_4$  as starting materials are shown in Fig. 9. The samples in the shape of polyhedrons consist of small and large particles.  $\text{LiNi}_{0.5}\text{Co}_{0.5}\text{O}_2$  has larger particles than  $\text{LiNi}_{0.7}\text{Co}_{0.3}\text{O}_2$ . The particles have quite flat surfaces.

The discharge capacity of  $\text{LiNi}_{0.9}\text{Co}_{0.1}\text{O}_2$  was lower than those of  $\text{LiNi}_{0.7}\text{Co}_{0.3}\text{O}_2$  and  $\text{LiNi}_{0.5}\text{Co}_{0.5}\text{O}_2$ . Fig. 10 presents

the variations of discharge capacity at 200  $\mu\text{A}/\text{cm}^2$  with the number of cycles for  $\text{LiNi}_{1-y}\text{Co}_y\text{O}_2$  ( $y = 0.3$  and 0.5) synthesized at 800 °C for 40 h using  $\text{LiOH}\cdot\text{H}_2\text{O}$ , NiO and  $\text{Co}_3\text{O}_4$  as starting materials. The first discharge capacities of  $\text{LiNi}_{0.5}\text{Co}_{0.5}\text{O}_2$  and  $\text{LiNi}_{0.7}\text{Co}_{0.3}\text{O}_2$  are 174.3 and 145.5 mAh/g, respectively. The cycling performance of  $\text{LiNi}_{0.7}\text{Co}_{0.3}\text{O}_2$  is better than  $\text{LiNi}_{0.5}\text{Co}_{0.5}\text{O}_2$ . Their discharge capacity fading rates of  $\text{LiNi}_{0.5}\text{Co}_{0.5}\text{O}_2$  and  $\text{LiNi}_{0.7}\text{Co}_{0.3}\text{O}_2$ , which were

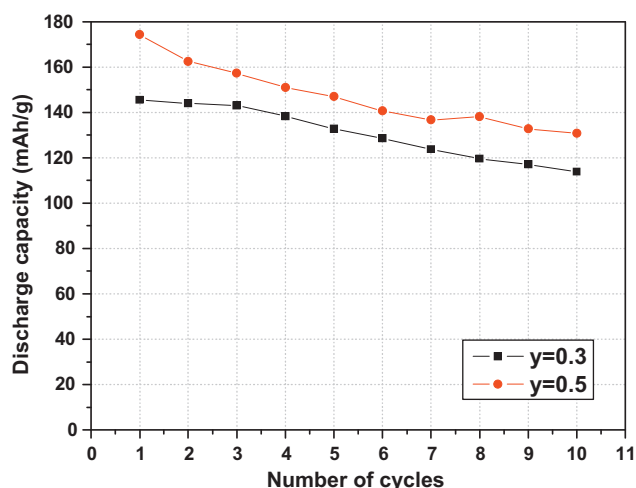


Fig. 10. Variations of discharge capacity at 200  $\mu\text{A}/\text{cm}^2$  with the number of cycles for  $\text{LiNi}_{1-y}\text{Co}_y\text{O}_2$  ( $y = 0.3$  and 0.5) synthesized at 800 °C for 40 h from  $\text{LiOH}\cdot\text{H}_2\text{O}$ , NiO and  $\text{Co}_3\text{O}_4$ .

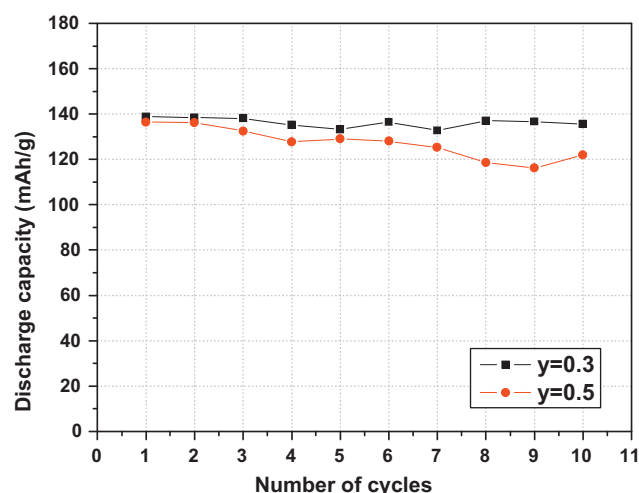


Fig. 11. Variations of discharge capacity at 200  $\mu\text{A}/\text{cm}^2$  with the number of cycles for  $\text{LiNi}_{1-y}\text{Co}_y\text{O}_2$  ( $y = 0.3$  and 0.5) synthesized at 750 °C for 40 h from  $\text{Li}_2\text{CO}_3$ , NiO and  $\text{Co}_3\text{O}_4$ .

Table 1

Comparison of  $\text{LiNi}_{1-y}\text{Co}_y\text{O}_2$  synthesized from  $\text{NiO}$ ,  $\text{Co}_3\text{O}_4$ , and  $\text{LiOH}\cdot\text{H}_2\text{O}$  or  $\text{Li}_2\text{CO}_3$ .

|              | $\text{LiOH}\cdot\text{H}_2\text{O}$ , $\text{NiO}$ and $\text{Co}_3\text{O}_4$   | $\text{Li}_2\text{CO}_3$ , $\text{NiO}$ and $\text{Co}_3\text{O}_4$  |
|--------------|---|--|
| Similarities | <ul style="list-style-type: none"> <li>• <math>\alpha\text{-NaFeO}_2</math> structure of the rhombohedral system (space group; <math>R\bar{3}m</math>).</li> <li>• <math>\text{Li}_2\text{CO}_3</math> peaks were observed at diffraction angles of <math>21^\circ</math> and <math>32^\circ</math> in the <math>\text{LiNi}_{0.9}\text{Co}_{0.1}\text{O}_2</math> samples.</li> <li>• Intensities of <math>\text{Li}_2\text{CO}_3</math> peaks decreased as the content of Co increased.</li> <li>• Particles grew as the synthesis time increased.</li> <li>• Particles grew as synthesis temperature increased in the same composition.</li> <li>• Particles grew a little larger as the content of Co increased at the same synthesis temperature.</li> </ul> |  |
| Differences  | <ul style="list-style-type: none"> <li>• The particle sizes of the samples from <math>\text{LiOH}\cdot\text{H}_2\text{O}</math>, <math>\text{NiO}</math> and <math>\text{Co}_3\text{O}_4</math> were relatively bigger than those from <math>\text{Li}_2\text{CO}_3</math>, <math>\text{NiO}</math> and <math>\text{Co}_3\text{O}_4</math> at all the temperatures and in all the compositions.</li> <li>• <math>\text{LiNi}_{0.5}\text{Co}_{0.5}\text{O}_2</math> calcined at <math>800^\circ\text{C}</math> had the largest first discharge capacity and <math>\text{LiNi}_{0.7}\text{Co}_{0.3}\text{O}_2</math> calcined at <math>800^\circ\text{C}</math> the best cycling performance.</li> </ul>  | <ul style="list-style-type: none"> <li>• <math>\text{LiNi}_{0.7}\text{Co}_{0.3}\text{O}_2</math> calcined at <math>800^\circ\text{C}</math> had the largest first discharge capacity and <math>\text{LiNi}_{0.7}\text{Co}_{0.3}\text{O}_2</math> calcined at <math>750^\circ\text{C}</math> exhibited the best cycling performance.</li> </ul> |

obtained from  $n = 1$  to  $n = 10$ , are 4.5 and 3.9 mAh/g/cycle, respectively.

The variations of discharge capacity at  $200\ \mu\text{A}/\text{cm}^2$  with the number of cycles for  $\text{LiNi}_{1-y}\text{Co}_y\text{O}_2$  ( $y = 0.3$  and  $0.5$ ) synthesized at  $750^\circ\text{C}$  for 40 h using  $\text{Li}_2\text{CO}_3$ ,  $\text{NiO}$  and  $\text{Co}_3\text{O}_4$  as starting materials are in Fig. 11. The first discharge capacities of  $\text{LiNi}_{0.7}\text{Co}_{0.3}\text{O}_2$  and  $\text{LiNi}_{0.5}\text{Co}_{0.5}\text{O}_2$  are 138.8 and 136.5 mAh/g, respectively. The cycling performance of  $\text{LiNi}_{0.7}\text{Co}_{0.3}\text{O}_2$  is better than  $\text{LiNi}_{0.5}\text{Co}_{0.5}\text{O}_2$ . The discharge capacities of  $\text{LiNi}_{0.7}\text{Co}_{0.3}\text{O}_2$  and  $\text{LiNi}_{0.5}\text{Co}_{0.5}\text{O}_2$  at  $n = 10$  are 135.6 and 122.0 mAh/g, respectively. Their discharge capacity fading rates are 0.3 and 2.1 mAh/g/cycle, respectively.

Fig. 12 shows the variations of discharge capacity at  $200\ \mu\text{A}/\text{cm}^2$  with the number of cycles for  $\text{LiNi}_{1-y}\text{Co}_y\text{O}_2$  ( $y = 0.3$  and  $0.5$ ) synthesized at  $800^\circ\text{C}$  for 40 h from  $\text{Li}_2\text{CO}_3$ ,  $\text{NiO}$  and  $\text{Co}_3\text{O}_4$ . The first discharge capacities of  $\text{LiNi}_{0.7}$

$\text{Co}_{0.3}\text{O}_2$  and  $\text{LiNi}_{0.5}\text{Co}_{0.5}\text{O}_2$  are 153.8 and 147.6 mAh/g, respectively. The cycling performance of  $\text{LiNi}_{0.5}\text{Co}_{0.5}\text{O}_2$  is better than  $\text{LiNi}_{0.7}\text{Co}_{0.3}\text{O}_2$ . The discharge capacities of  $\text{LiNi}_{0.5}\text{Co}_{0.5}\text{O}_2$  and  $\text{LiNi}_{0.7}\text{Co}_{0.3}\text{O}_2$  at  $n = 6$  are 141.9 and 122.7 mAh/g, respectively. Their discharge capacity fading rates are 1.3 and 6.3 mAh/g/cycle, respectively.

Table 1 compares the physical and electrochemical properties of  $\text{LiNi}_{1-y}\text{Co}_y\text{O}_2$  synthesized from  $\text{NiO}$ ,  $\text{Co}_3\text{O}_4$ , and  $\text{LiOH}\cdot\text{H}_2\text{O}$  or  $\text{Li}_2\text{CO}_3$ . The particle size increases, on the whole, as the synthesis temperature increases and as the Co content increases. The particle sizes of the  $\text{LiNi}_{1-y}\text{Co}_y\text{O}_2$  specimens synthesized at all three temperatures from  $\text{Li}_2\text{CO}_3$ ,  $\text{NiO}$  and  $\text{Co}_3\text{O}_4$  are larger than those of the specimens synthesized from  $\text{LiOH}\cdot\text{H}_2\text{O}$ ,  $\text{NiO}$  and  $\text{Co}_3\text{O}_4$  for all of the compositions. Among  $\text{LiNi}_{1-y}\text{Co}_y\text{O}_2$  ( $y = 0.1, 0.3$  and  $0.5$ ) synthesized from  $\text{LiOH}\cdot\text{H}_2\text{O}$ ,  $\text{NiO}$  and  $\text{Co}_3\text{O}_4$ ,  $\text{LiNi}_{0.5}\text{Co}_{0.5}\text{O}_2$  calcined at  $800^\circ\text{C}$  had the largest first discharge capacity and  $\text{LiNi}_{0.7}\text{Co}_{0.3}\text{O}_2$  calcined at  $800^\circ\text{C}$  the best cycling performance. Among  $\text{LiNi}_{1-y}\text{Co}_y\text{O}_2$  ( $y = 0.1, 0.3$  and  $0.5$ ) synthesized from  $\text{Li}_2\text{CO}_3$ ,  $\text{NiO}$  and  $\text{Co}_3\text{O}_4$ ,  $\text{LiNi}_{0.7}\text{Co}_{0.3}\text{O}_2$  calcined at  $800^\circ\text{C}$  had the largest first discharge capacity and  $\text{LiNi}_{0.7}\text{Co}_{0.3}\text{O}_2$  calcined at  $750^\circ\text{C}$  exhibited the best cycling performance.

Among  $\text{LiNi}_{1-y}\text{Co}_y\text{O}_2$  ( $y = 0.1, 0.3$  and  $0.5$ ) synthesized for 40 h from  $\text{LiOH}\cdot\text{H}_2\text{O}$ ,  $\text{NiO}$  and  $\text{Co}_3\text{O}_4$ , and from  $\text{Li}_2\text{CO}_3$ ,  $\text{NiO}$  and  $\text{Co}_3\text{O}_4$ ,  $\text{LiNi}_{0.5}\text{Co}_{0.5}\text{O}_2$  synthesized from  $\text{Li}_2\text{CO}_3$ ,  $\text{NiO}$  and  $\text{Co}_3\text{O}_4$  at  $800^\circ\text{C}$  has relatively large first discharge capacity and relatively good cycling performance. This sample is considered the best one with relatively good electrochemical properties.

#### 4. Conclusions

$\text{LiNi}_{1-y}\text{Co}_y\text{O}_2$  ( $y = 0.1, 0.3$  and  $0.5$ ) were synthesized by the solid-state reaction method at  $750^\circ\text{C}$ ,  $800^\circ\text{C}$  and  $850^\circ\text{C}$  from  $\text{LiOH}\cdot\text{H}_2\text{O}$ ,  $\text{NiO}$  and  $\text{Co}_3\text{O}_4$  and from  $\text{Li}_2\text{CO}_3$ ,  $\text{NiO}$  and  $\text{Co}_3\text{O}_4$ .

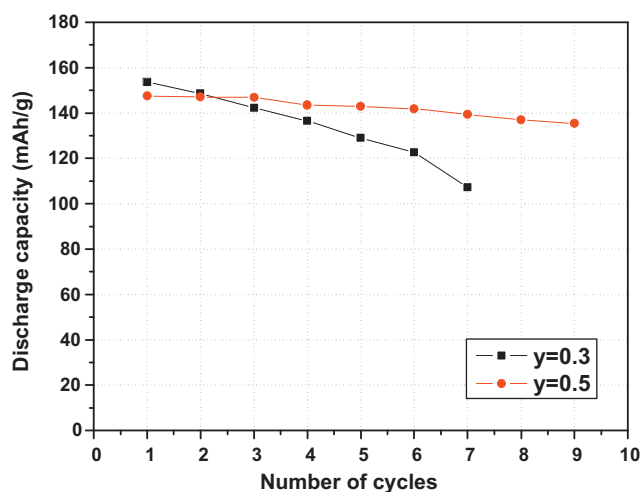


Fig. 12. Variations of discharge capacity at  $200\ \mu\text{A}/\text{cm}^2$  with the number of cycles for  $\text{LiNi}_{1-y}\text{Co}_y\text{O}_2$  ( $y = 0.3$  and  $0.5$ ) synthesized at  $800^\circ\text{C}$  for 40 h from  $\text{Li}_2\text{CO}_3$ ,  $\text{NiO}$  and  $\text{Co}_3\text{O}_4$ .

$\text{LiNi}_{1-y}\text{Co}_y\text{O}_2$  synthesized from different starting materials had same similarities; they had  $\alpha\text{-NaFeO}_2$  structure of the rhombohedral system (space group;  $R\bar{3}m$ ).  $\text{Li}_2\text{CO}_3$  peaks were observed at diffraction angles of  $21^\circ$  and  $32^\circ$  in the  $\text{LiNi}_{0.9}\text{Co}_{0.1}\text{O}_2$  samples. The intensities of  $\text{Li}_2\text{CO}_3$  peaks decreased as the content of Co increased. The particles grew as the synthesis time and temperature increased. They had some differences; the particle sizes of the samples from  $\text{LiOH}\cdot\text{H}_2\text{O}$ , NiO and  $\text{Co}_3\text{O}_4$  were relatively bigger than those from  $\text{Li}_2\text{CO}_3$ , NiO and  $\text{Co}_3\text{O}_4$  at all the temperatures and in all the compositions.

Among  $\text{LiNi}_{1-y}\text{Co}_y\text{O}_2$  ( $y = 0.1, 0.3$  and  $0.5$ ) synthesized for 40 h from  $\text{LiOH}\cdot\text{H}_2\text{O}$ , NiO and  $\text{Co}_3\text{O}_4$ , and from  $\text{Li}_2\text{CO}_3$ , NiO and  $\text{Co}_3\text{O}_4$ ,  $\text{LiNi}_{0.5}\text{Co}_{0.5}\text{O}_2$  synthesized from  $\text{Li}_2\text{CO}_3$ , NiO and  $\text{Co}_3\text{O}_4$  at  $800^\circ\text{C}$  has relatively large first discharge capacity and relatively good cycling performance. This sample is considered the best one with relatively good electrochemical properties.

The intensity ratio,  $I_{003}/I_{104}$ , increases as the Co content increases. The unit cell volumes of the samples synthesized at the same temperature decrease as the Co content increases. These two results indicate that the degree of displacement of the nickel and lithium ions decreases as the Co content increases.

## References

- [1] K. Ozawa, Lithium-ion rechargeable batteries with  $\text{LiCoO}_2$  and carbon electrodes: the  $\text{LiCoO}_2/\text{C}$  system, *Solid State Ionics* 69 (1994) 212–221.
- [2] R. Alcántara, P. Lavela, J.L. Tirado, R. Stoyanova, E. Zhecheva, Structure and electrochemical properties of boron-doped  $\text{LiCoO}_2$ , *Journal of Solid State Chemistry* 134 (1997) 265–273.
- [3] Z.S. Peng, C.R. Wan, C.Y. Jiang, Synthesis by sol–gel process and characterization of  $\text{LiCoO}_2$  cathode materials, *Journal of Power Sources* 72 (1998) 215–220.
- [4] S.N. Kwon, J.H. Song, D.R. Mumm, Effects of cathode fabrication conditions and cycling on the electrochemical performance of  $\text{LiNiO}_2$  synthesized by combustion and calcination, *Ceramics International* 37 (5) (2011) 1543–1548.
- [5] J.R. Dahn, U. von Sacken, C.A. Michal, Structure and electrochemistry of  $\text{Li}_{1\pm y}\text{NiO}_2$  and a new  $\text{Li}_2\text{NiO}_2$  phase with the  $\text{Ni}(\text{OH})_2$  structure, *Solid State Ionics* 44 (1990) 87–97.
- [6] J.R. Dahn, U. von Sacken, M.W. Juskow, H. Al-Janaby, Rechargeable  $\text{LiNiO}_2$ /carbon cells, *Journal of Electrochemical Society* 138 (1991) 2207–2212.
- [7] D.H. Kim, Y.U. Jeong, Crystal structures and electrochemical properties of  $\text{LiNi}_{1-x}\text{Mg}_x\text{O}_2$  ( $0 \leq x \leq 0.1$ ) for cathode materials of secondary lithium batteries, *Korean Journal of Metals and Materials* 48 (3) (2010) 262–267.
- [8] M.Y. Song, D.R. Mumm, C.K. Park, H.R. Park, Cycling performances of  $\text{LiNi}_{1-y}\text{M}_y\text{O}_2$  ( $\text{M} = \text{Ni}, \text{Ga}, \text{Al}$  and/or  $\text{Ti}$ ) synthesized by wet milling and solid-state method, *Metals and Materials International*, <http://dx.doi.org/10.1007/s12540-012-3013-3>, in press.
- [9] J.M. Tarascon, E. Wang, F.K. Shokoohi, W.R. Mckinnon, S. Colson, The spinel phase of  $\text{LiMn}_2\text{O}_4$  as a cathode in secondary lithium cells, *Journal of Electrochemical Society* 138 (1991) 2859–2864.
- [10] M.Y. Song, D.S. Ahn, On the capacity deterioration of spinel phase  $\text{LiMn}_2\text{O}_4$  with cycling around 4 V, *Solid State Ionics* 112 (1998) 21–24.
- [11] M.Y. Song, D.S. Ahn, H.R. Park, Capacity fading of spinel phase  $\text{LiMn}_2\text{O}_4$  with cycling, *Journal of Power Sources* 83 (1999) 57–60.
- [12] D.S. Ahn, M.Y. Song, Variations of the electrochemical properties of  $\text{LiMn}_2\text{O}_4$  with synthesis conditions, *Journal of Electrochemical Society* 147 (3) (2000) 874–879.
- [13] H.J. Guo, Q.H. Li, X.H. Li, Z.X. Wang, W.J. Peng, Novel synthesis of  $\text{LiMn}_2\text{O}_4$  with large tap density by oxidation of manganese powder, *Energy Conversion and Management* 52 (4) (2011) 2009–2014.
- [14] C. Wan, M. Cheng, D. Wu, Synthesis of spherical spinel  $\text{LiMn}_2\text{O}_4$  with commercial manganese carbonate, *Powder Technology* 210 (1) (2011) 47–51.
- [15] J.W. Park, J.H. Yu, K.W. Kim, H.S. Ryu, J.H. Ahn, C.S. Jin, K.H. Shin, Y.C. Kim, H.J. Ahn, Surface morphology changes of lithium/sulfur battery using multi-walled carbon nanotube added sulfur electrode during cyclings, *Korean Journal of Metals and Materials* 49 (2) (2011) 174–179.
- [16] Y. Nishida, K. Nakane, T. Satoh, Synthesis and properties of gallium-doped  $\text{LiNiO}_2$  as the cathode material for lithium secondary batteries, *Journal of Power Sources* 68 (1997) 561–564.
- [17] P. Barboux, J.M. Tarascon, F.K. Shokoohi, The use of acetates as precursors for the low-temperature synthesis of  $\text{LiMn}_2\text{O}_4$  and  $\text{LiCoO}_2$  intercalation compounds, *Journal of Solid State Chemistry* 94 (1991) 185–196.
- [18] J. Morales, C. Perez-Vicente, J.L. Tirado, Cation distribution and chemical deintercalation of  $\text{Li}_{1-x}\text{Ni}_{1+x}\text{O}_2$ , *Material Research Bulletin* 25 (1990) 623–630.
- [19] A. Rougier, I. Saadoun, P. Gravereau, P. Willmann, C. Delmas, Effect of cobalt substitution on cationic distribution in  $\text{LiNi}_{1-y}\text{Co}_y\text{O}_2$  electrode materials, *Solid State Ionics* 90 (1996) 83–90.
- [20] B.J. Neudecker, R.A. Zuh, B.S. Kwak, J.B. Bates, J.D. Robertson, Lithium manganese nickel oxides  $\text{Li}_x(\text{Mn}_y\text{Ni}_{1-y})_{2-x}\text{O}_2$ , *Journal of Electrochemical Society* 145 (1998) 4148–4157.
- [21] C. Delmas, I. Saadoun, Electrochemical and physical properties of the  $\text{Li}_x\text{Ni}_{1-y}\text{Co}_y\text{O}_2$  phases, *Solid State Ionics* 53–56 (1992) 370–375.
- [22] E. Zhecheva, R. Stoyanova, Stabilization of the layered crystal structure of  $\text{LiNiO}_2$  by Co-substitution, *Solid State Ionics* 66 (1993) 143–149.
- [23] C. Delmas, I. Saadoun, A. Rougier, The cycling properties of the  $\text{Li}_x\text{Ni}_{1-y}\text{Co}_y\text{O}_2$  electrode, *Journal of Power Sources* 43–44 (1993) 595–602.
- [24] A. Ueda, T. Ohzuku, Solid-state redox reactions of  $\text{LiNi}_{1/2}\text{Co}_{1/2}\text{O}_2$  ( $R\bar{3}m$ ) for 4 volt secondary lithium cells, *Journal of Electrochemical Society* 141 (1994) 2010–2014.
- [25] M. Menetrier, A. Rougier, C. Delmas, Cobalt segregation in the  $\text{LiNi}_{1-y}\text{Co}_y\text{O}_2$  solid solution: a preliminary  $^7\text{Li}$  NMR study, *Solid State Communications* 90 (1994) 439–442.
- [26] K. Kubo, S. Arai, S. Yamada, M. Kanda, Synthesis and charge–discharge properties of  $\text{Li}_{1+x}\text{Ni}_{1-x-y}\text{Co}_y\text{O}_{2-z}\text{F}_z$ , *Journal of Power Sources* 81–82 (1999) 599–603.
- [27] H.U. Kim, D.R. Mumm, H.R. Park, M.Y. Song, Synthesis by a simple combustion method and electrochemical properties of  $\text{LiCo}_{1/3}\text{Ni}_{1/3}\text{Mn}_{1/3}\text{O}_2$ , *Electronic Materials Letters* 6 (3) (2010) 91–95.
- [28] S.H. Ju, J.H. Kim, Y.C. Kang, Electrochemical properties of  $\text{LiNi}_{0.8}\text{Co}_{0.2-x}\text{Al}_x\text{O}_2$  ( $0 \leq x \leq 0.1$ ) cathode particles prepared by spray pyrolysis from the spray solutions with and without organic additives, *Metals and Materials International* 16 (2) (2010) 299–303.
- [29] M.Y. Song, H. Rim, E.Y. Bang, Electrochemical properties of cathode materials  $\text{LiNi}_{1-y}\text{Co}_y\text{O}_2$  synthesized using various starting materials, *Journal of Applied Electrochemistry* 34 (2004) 383–389.
- [30] T. Ohzuku, A. Ueda, M. Nagayama, Electrochemistry and structural chemistry of  $\text{LiNiO}_2$  ( $R\bar{3}m$ ) for 4 volt lithium cells, *Journal of Electrochemical Society* 140 (1993) 1862–1870.